INTERNATIONAL JOURNAL OF MARITIME TECHNOLOGY

IJMT Vol.13/ Winter 2020 (1-9)

Available online at: www. ijmt.ir

Investigation the effect of Land Characteristics on Hurricane Freshwater Flood Vulnerability

Mehdi Rezapour [1*], Tom Baldock[2]

[1] *Assistant professor, Chabahar Maritime University, rezapour@cmu.ac.ir*
[2] *School of Civil Engineering, University of Queensland, St Lucia, QLD, 4072, Australia, baldock@uq.edu.au*

ARTICLE INFO

Article History:
Received: 03 Nov. 2019
Accepted: 27 Jan. 2020

Keywords:
Tropical Cyclone
Hurricane Hazard
Risk Index
Land Characteristics
Social factors

ABSTRACT

This study analyses two comparison examples (hurricanes Frances versus Jeanne and hurricanes Rita versus Irene) to account for the catchment characteristics and social factors for the area impacted by the track of a tropical cyclone. This will result in a way of categorizing tropical cyclone, which can be combined with the previous meteorological indexes to better assess the potential impact of each tropical cyclone from a hazard mitigation and the disaster response perspective. Given that the highest correlation between fatalities and damage occurs for the rainfall index TCRI, vulnerability to rainfall was selected as the focus of the research. The results show that the impacted areas and the population who lives in the impacted areas are two important indicators of flood vulnerability. The new index (TRI) yields a lower RMSE in rank position, at 3.5 and 2.2, compared with the SSHE at 5.8 and 5.7 for selected hurricane damage and death toll, respectively.

1.Introduction

Although coastal zones are attractive for people to live, they are impacted by different natural phenomena, mostly of hydro-meteorological origin, such as waves, wind, tides, and rainfall, which can reach extraordinary magnitudes during the occurrence of severe events such as Tropical Cyclones (a generic term for a Hurricane, Typhoon or tropical storm) and tsunami. The direct consequences of these extreme events are flooding (caused by sea-level rise, surge and rainfall) and beach erosion (due to an increase in current velocities and wave energy). A combination of these causes land loss, damage to infrastructure and natural habitats, ecological imbalance, health problems in the population and instability in economic activities [1-3]. Interestingly, the risk of living in these areas is increasing in parallel with the growing population and wealth of these regions [4]. The available literature dealing with coastal risk assessment is quite wide, focusing mainly on the risk of loss resulting directly from the occurrence of extreme natural events [1].

Peduzzi et al. (2012a) contend that the number of exposed people and the vulnerability along with the intensity and frequency of storms determine the level of impact of tropical cyclones on humans. They presented a new methodology based on physically observed events and related contextual parameters to take into account the cumulative effects of climate change [4]. They analyzed mortality-risk trend from 1970-2010 to predict the Tropical-Cyclone Mortality-Risk Index (TC-MRI) by 2030. Dao and Peduzzi (2004) introduce the Disaster Risk Index (DRI) to improve understanding of the relationship between development and disaster risk at the global level. The primary assumption behind the index is that differences in risk levels of countries with similar exposures to natural hazards are described by socio-economic factors, i.e. by the population vulnerability. The DRI allows the measurement and the comparison of relative levels of risk, exposure to risk and vulnerability by country basis [5]. This method concentrates on the evaluation of risk for four hazards(floods, droughts, earthquakes, and cyclones). Davidson and Lambert (2001) describe the Hurricane Disaster Risk Index (HDRI) of U.S. coastal Counties. It was developed to be as an easily understandable tool that can be applied to compare the risk of life and economic loss in different coastal counties in the United States, as well as to compare the different relative contributions of various factors, e.g., the frequency of hurricanes and the quality

[DOR: 20.1001.1.23456000.2020.13.0.4.6]

of the emergency evacuation plan. The HDRI is developed to support local, state, and national government agencies as they make resource allocation decisions, make high-level planning decisions, and raise public awareness of hurricane risk [6]. The HAZUZ-MH Hurricane Model uses five model components comprising a (hazard model, a terrain model (to classify terrain by roughness value), a wind load model, a physical damage model, and a loss model) (Vickery et al., 2006a, Vickery et al., 2006b). The HAZUZ-MH model estimates the possibility of damage and loss to buildings from wind storm and storm surge. The model makes use of an existing wind field model and sea surface temperature as the boundary layer and computes wind speed as a function of central pressure, storm transition speed and surface roughness.

Although there is a lot of evidence that shows that considerable damage and a high number of fatalities arising from floods caused by either torrential rainfall, storm surge or a combination of both, there is no scale to predict the likely magnitude of such damage and fatalities. A new methodology can improve the indexes by assessing the important land characteristics as the second significant component when tropical cyclones make landfall.

2. Methodology and Databases

The impact of rainfall within the catchment has been divided into three main steps (Figure 2.1); the transformation of rainfall into a runoff; the resulting flood flows corresponding to the runoff and the losses arising from the flood flows.

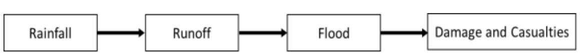

Figure 2.1: physical process steps to determine the influence of catchment characteristics within a vulnerability index.

The vulnerability is a product of the hazards and exposure to the hazards [7]. Consequently, to develop a rainfall vulnerability index, it is necessary to firstly identify the effective factors, secondly to create indicators that represent the effects of the selected factors and finally to develop a mathematical equation for those indicators as an index [6], illustrated in Figure 2.2. The combination of both sets of process steps in the case of a rainfall vulnerability index is then a flowchart of the form shown in Figure 2.3.

Figure 2.2: Process steps to develop a general index.

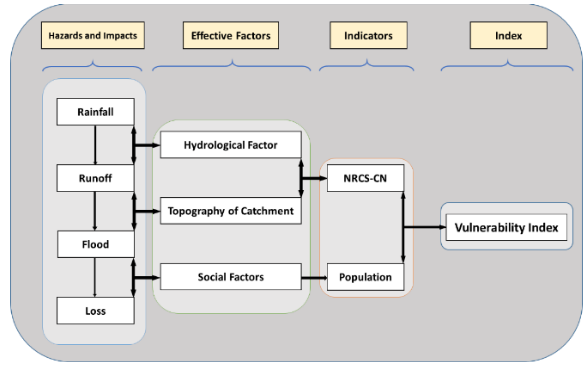

Figure 2.3: Conceptual framework for calculating the Vulnerability Index.

The USDA Natural Resources Conservation Service (NRCS) Curve Number (CN) was selected as the key indicator of the Hydrological and topographical characteristics of the selected rainfall affected areas. The areas with more than 5 inches [127 mm] total rainfall, resulting from a given hurricane, were considered as the impacted areas. Thus, the impacted population is the population living in the impacted areas. The impacted population and subgroups such as age range, gender, poverty, have been considered previously for the purpose of estimating an exposure indicator, e.g. to compute the Hurricane Disaster Risk Index (HDRI;[6]). Those data were obtained from county emergency management departments or local or state census. The land value of the impacted area has also been used previously for estimating an economic vulnerability indicator [6]. In this study, the total population of each impacted area was chosen as the simplest indicator of exposure, representing the social characteristics of the area [8]. The methodology used for calculating the given indicators is as follows:

1: Derive impacted areas, which are the areas with more than 5 inches [127 mm] total.

2: Generate the land use map, soil type map, DEMs grid map and the population grid map for the impacted areas.

3: Calculate the weighted NRCS-CN and total population (exposure) for each hurricane.

2.1. Justification of the NRCS-CN as the indicator

The NRCS method that indicates the capability of the catchment to control the received rainfall is widely used in many commonly standard hydrological models [9-12], including the Hydrologic Modelling System (HEC-HMS), the Erosion Productivity Impact Calculator (EPIC), and the Agricultural Non-Point Source Pollution model (AGNPS). The NRCS-CN classifies catchments according to their hydrological soil groups and land cover types[13].

2.2. Application within HEC-GeoHMS

The CN Grid tool within HEC-GeoHMS has been used for generating curve number gridded maps, by means of a merged layer from both land use and soil type layers in a given area, together with a filled sink DEM layer (users should use the fill sinks tool to remove potential sinks generated from the reconditioning process) and a LookUp table. The LookUp table relates to land use and hydrological soil groups to a curve number, as indicated in Table 2.1. Figure 2.4 shows a schematic illustration of the process steps required to generate each CN grid map. An example of a CN grid map is shown later in Figure 4.2.

Table 2.1: Example curve number Look Up table.

Land use value	Land Use	Hydrological Soil Type			
		A	B	C	D
1	Water	100	100	100	100
2	Residential	57	72	81	86
3	Forest	30	58	71	78
4	Agricultural	67	77	83	87

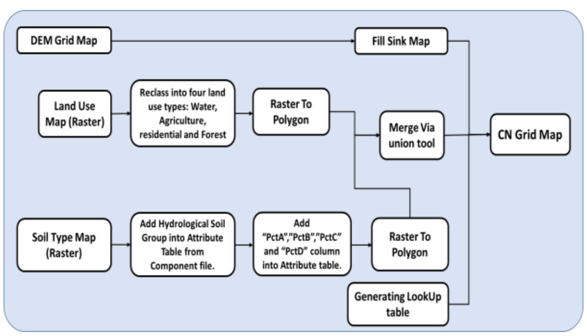

Figure 2.4: Conceptual framework for generating NRCS-CN maps.

2.3. Land Databases

2.3.1. Land Use Map

The NCLD 2011 is the latest version available and is designed for general users from biology and climate to hydrology and risk analysis. Figure 2.5 shows a sample NCLD 2011 image related to an area of 49,203 $(km)^2$ impacted by hurricane Rita (2005).

Table 2.2: 16 NCLD 2011 different land use classes [14].

Class	Classification Description	Reclassifying
11	Open Water	Water
21	Developed, Open Space	Residential
22	Developed, Low Intensity	Residential
23	Developed, Medium Intensity	Residential
24	Developed, High Intensity	Residential
31	Barren land (Rock/Sand/Clay)	Agricultural
41	Deciduous Forest	Forest
42	Evergreen Forest	Forest
43	Mixed Forest	Forest
52	Shrub/Scrub	Agricultural
71	Grassland/Herbaceous	Agricultural
81	Pasture/Hay	Agricultural
82	Cultivated Crops	Agricultural
90	Woody Wetland	Water
95	Emergent Herbaceous Wetland	Water
No Data	----------	----------

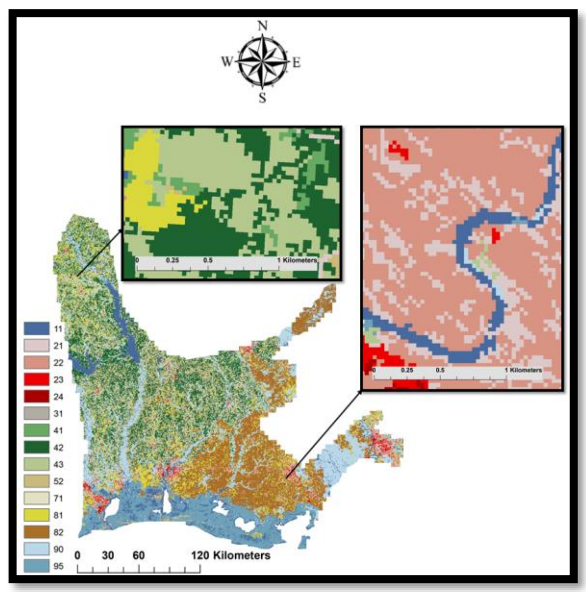

Figure 2.5: Sample of extracted land use map for a small region impacted by Hurricane Rita (2005). Data from NLCD 2011.

2.3.2. Soil Type Map

The Gridded Soil Survey Geographic (gSSURGO) database that was used in this study is derived from the Soil Survey Geographic (version 2.2) database dated December 1, 2014. These data were amended by merging the SSURGO digital vector map with the tabular data into a state-wide gridded map layer derived from the vector map, with the new value added to a lookup (value) table. Figure 2.6 illustrates an extracted soil type map for a region impacted by Hurricane Rita (2005).

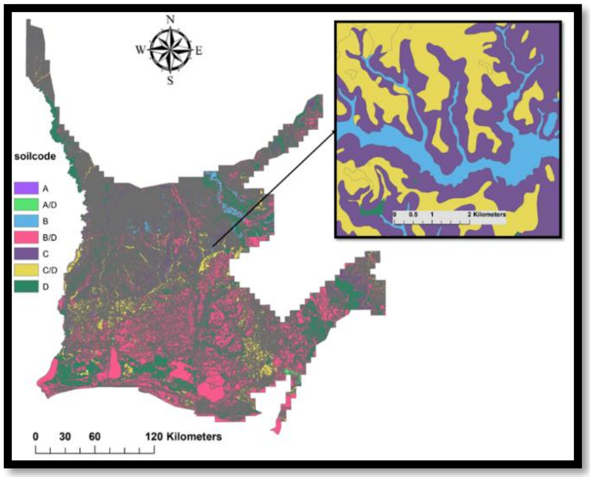

Figure 2.6: Sample of extracted soil type map for a small region impacted by Hurricane Rita (2005). Data from gSSURGO.

The soil types are categorized hydrologically, based on their estimated of runoff potential (e.g. soils with high infiltration rate have a low runoff potential, and vice versa). Soils are divided into four different types (A, B, C, and D) corresponding to their water infiltration rates under the assumption of no protection by vegetation, thoroughly wet, receiving long-duration precipitation. The soil types in the United States are divided into three further classes (A/D, B/D, and C/D). The first letter is for drained areas and the second for undrained areas. All areas are assumed drained in HEC-GeoHMS for simplicity.

2.3.3. Population Database

The Gridded Population of the World, Version 3 (GPWv3) was selected to quantify the population in the impacted areas. The GPWv3 describes the distribution of human population across the world, transforming population census data (according to irregular census blocks and block group boundaries), which most countries collect for sub-national administrative units, into a regular raster-grid. GPWv3 gives the estimation of total population and population density for each cell, corresponding to the normal boundaries of the grid and the overlap between the irregular boundaries of administrative units [15]. The GPWv3 layer for the continental U.S.A. has been used in this study and is illustrated in Figure 2.7.

Figure 2.7: U.S population map (GPWv3) with 2.5 arc-minutes resolution, or roughly 5 km at the equator.

2.3.4. DEM Grid Map

The Shuttle Radar Topographic Mission (STRM) 30m Digital Elevation Data for the continental U.S.A was chosen as the DEM for the study. The STRM, produced by NASA, is a major breakthrough in digital mapping of the globe, and provides a major advance in the availability of high-quality elevation data for large portions of the tropical regions and other areas of the developing world. The NASA Shuttle Radar Topographic Mission (STRM) has provided digital elevation data (DEMs) for over 80% of the globe with a resolution of 90m. However, STRM data with 30m resolution is available in the continental U.S.A. and is used for the purposes of this study [16], (Figure 2.8).

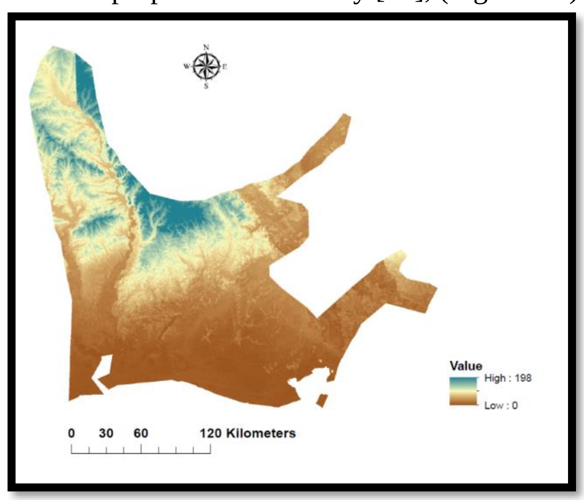

Figure 2.8: Sample of extracted DEM grid map for a small region impacted by Hurricane Rita (2005). Data from STRM 30m.

2.3.5. Total Rainfall Map

The impacted areas for each storm have been extracted using the total rainfall map provided by Weather Prediction Center (WPC). The Weather Prediction Center has constructed the total rainfall map using data from National Weather Service, River Forecast Centers, and National Hurricane Center reports.The map yields derived areas with more than 5 inches [127mm] total

[DOR: 20.1001.1.23456000.2020.13.0.4.6]

rainfall as the impacted areas. Czajkowski et al. (2011) show that the total rainfall and predicted fatalities have the exponential relation, with fatalities starting to occur in areas with more than 5 inches total rainfall (Figure 2.9). Figure 2.10 shows the total rainfall for hurricane Rita[17].

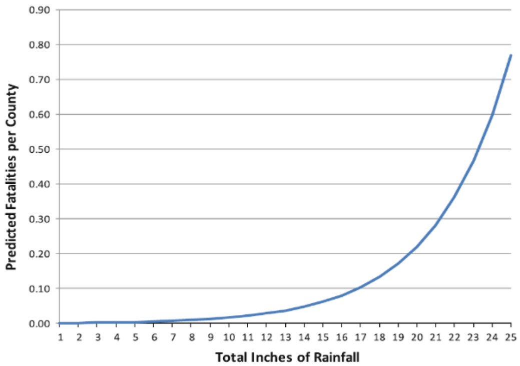

Figure 2.9: The relation between predicted fatalities with the total rainfall, [17].

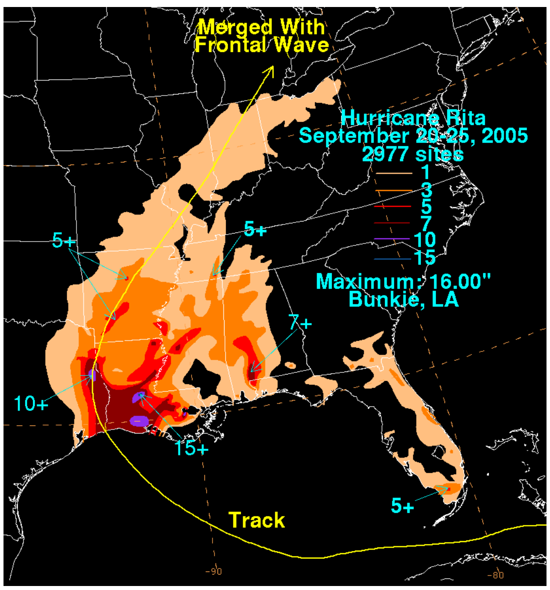

Figure 2.10: Hurricane Rita total rainfall map, National Hurricane Centre, NOAA.

3. Hurricane Jeanne versus hurricane Frances (impact of land characteristics)

Category 2 (based on the SSHS) hurricane Frances(2004) caused 12 billion U.S. dollar worth of damage and led to 49 fatalities, compared with category 3 Hurricane Jeanne (2004), with 7 billion USD of damage and 5 fatalities, in the United States, even though both made landfall at almost the same location, just 2 miles apart in Florida (Matyas and Cartaya 2009; Table 3.1, Figure 3.1 and 3.2). Further, the other existing hurricane scales such as SSHS, HII, HHI, and HSI also do not classify properly the differing impact of these hurricanes (Table 3.1).

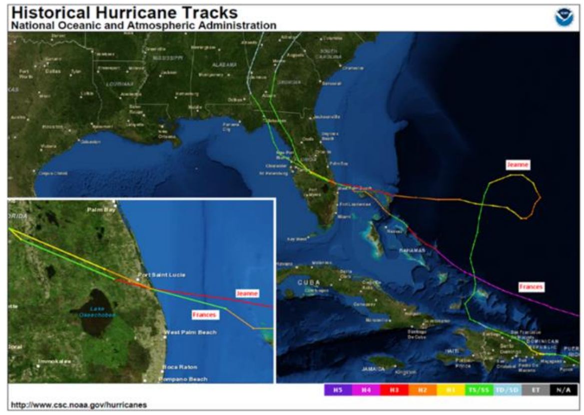

Figure 3.1: Tracks of Hurricane Jeanne and Hurricane Frances; http://www.csc.noaa.gov/hurricanes**.**

Table 3.1: A comparison of the characteristics and existing hazard scales for Hurricane Frances (2004) and Hurricane Jeanne (2004).

Characteristics	Frances (2004)	Jeanne (2004)	Note
Sustained wind (kt)	90	105	At landfall
Radius of max wind (n mi)	29	39	At landfall
Forward Speed (kt)	10	10.5	At landfall
Max surge (ft)	6	5-6	
Landfall location	Florida	Florida	(2 mi apart)
U.S. damage (billion USD)	12	7	2004 values
U.S. death toll	49	5	
SSHS	2	3	
HII	2	2.7	Kantha (2006)
HHI	5.1	7.5	Kantha (2006)
HSI	26	29	Hebert et al. (2010)

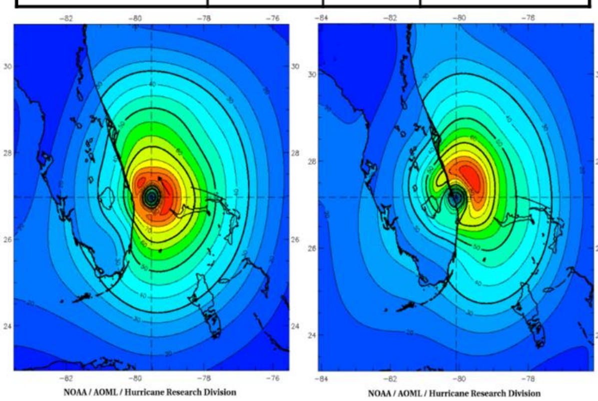

Figure 3.2: A comparison of the wind field (kt) from (left) category 3 Hurricane Jeanne and (right) category 2 Hurricane Frances, (Source: NOAA/AOML/HRD.)

To consider these two systems in more detail and, firstly the areas with more than five inches total rainfall (impacted areas) for hurricanes Jeanne and Frances were identified (Figures 3.3). The land use and soil type polygon layers were then generated for the impacted areas using Arcmap10.1. The gridded curve number maps of the impacted areas of each hurricane were subsequently generated using the framework.

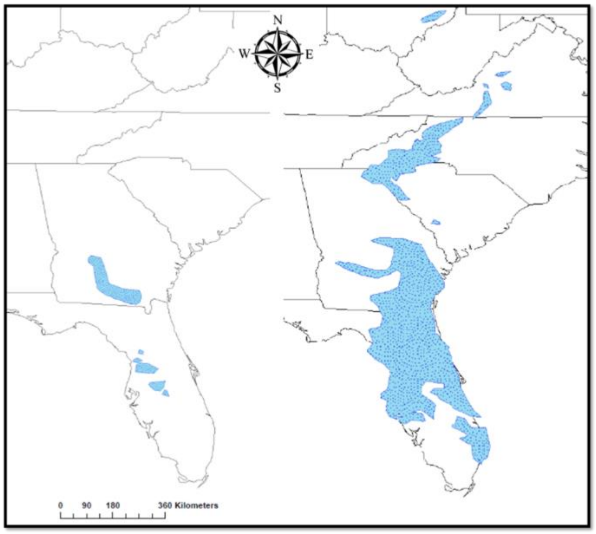

Figure 3.3: Hurricane Frances (2004) impacted areas (right dotted blue areas) versus Hurricane Jeanne (2004) impacted areas (left dotted blue areas).

For the land characteristics, the results show that the impacted area Curve Number of hurricane Frances and Jeanne are approximately the same, 74 versus 77, respectively (Table 3.2) which is logically predictable due to their similar trajectory, i.e. both hurricanes impacted catchments with the same soil type and land use.

The question is then, what is the reason for the differences between the damage rate and death toll caused by Frances and Jeanne if they both impacted land with the same Curve Number? Despite some differences between their rainfall characteristics, such as their rainfall intensity, rainfall distribution, and rainfall duration, another reason might be due to differences in their impacted population. Hurricane Frances affected more than 11 million residents with a population density of 130 people per square kilometer versus approximately half a million people with a population density of 32 people per square kilometer for hurricane Jeanne (Table 6.2).

Table 3.2: Hurricane Jeanne (2005) and hurricane Frances estimated polygon areas, population and Curve Number.

Hurricane Jeanne 2005			
Polygon Number	Area(A) km^2	Curve Number	Population
1	8885	78.1	41,905
2	174	61.1	10,118
3	287	55.3	33,826
4	1850	70	74,673
5	114	77.8	219,795
6	252	69.7	17,199
7	1663	82.6	56,187
Total	14251	76.8	453,703

Hurricane Frances 2005				
Polygon Number		Area(A) km^2	Curve Number	Population
1		36779	75.9	2,276316
2	1	62400	79.5	7,705,617
	2		78.2	
3		268	64.8	5,374
4	1	18140	64.3	1,222,865
	2		68.3	
	3		63.2	
5		1405	65.8	112,736
6		139	71.2	5,420
7		545	64.3	49,977
8		339	68.3	3,816
9		820	74	11,213
Total		87738	73.7	11,393,334

4. Hurricane Rita (2005) versus hurricane Irene (2011)

The characteristics of CAT2 hurricane Irene and CAT3 hurricane Rita are compared in Table 4.1. The U.S.A National Hurricane Centre (NHC) reports show that for hurricane Irene 21 out of the 42 fatalities were caused by freshwater flooding, compared with hurricane Rita with only one freshwater flooding fatality out of all 7 direct fatalities. Direct deaths are death caused by the environmental force of the hurricane (e.g., wind or flood) or by the direct consequences of these forces (e.g., structural collapse). Indirect deaths are defined as deaths occurring in a situation in which the hurricane led to unsafe conditions (e.g., hazardous roads) or caused a loss or disruption of usual services that contributed to the death (e.g., loss of electrical services). The NRCS-CN grid maps for both hurricanes have been calculated for their respective impacted areas. The total impacted areas (Figure 4.1) for Irene and Rita are 82,182 km^2 and 51,805 km^2 respectively (Table 4.1). Adopting the methodology, the calculated weighted averaged Curve Number for Rita is 85, against 78 for Irene (Figure 4.2). This indicates that the areas impacted by Rita have greater runoff potential than Irene. However, ignoring any differences in emergency management decisions and evacuation systems, the degree of exposure might also be the reason for the difference in fatalities. Hurricane Irene impacted more than 19 million residents, versus 1.6 million people affected by hurricane Rita (Table 4.1).

[DOR: 20.1001.1.23456000.2020.13.0.4.6]

Table 4.1: A comparison of the characteristics of hurricanes Rita (2005) and Irene (2011).

NO	Characteristics	Rita (2005)	Irene (2011)	Note
1	Sustained wind (kt)	96	80	At landfall
2	Radius of max wind (n mi)	16	20	At landfall
3	Forward Speed (kt)	16	32	At landfall
5	Landfall location	Between Texas and Louisiana	North Carolina	
6	SSHS	3	2	
6	U.S. damage (billion USD)	14.3	16.1	2013 USD
7	Fresh water flooding death toll	1	21	
13	Impacted area $(km)^2$	51,805	82,182	
14	Impacted population	1,642,000	19,672,000	
15	Curve Number	84	78	

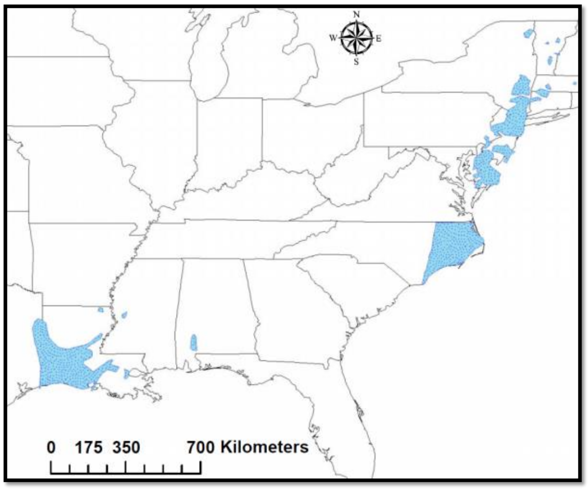

Figure 4.1: Hurricane Rita (2005) impacted areas (dotted blue areas in the Gulf of Mexico and hurricane Irene (dotted blue areas on the east coast).

The impacted population has been plotted against the square tropical cyclone rainfall index, which is called the Total Rainfall Index (TRI) in this study (Figure 4.3). Logically, the vulnerability to selected hurricanes should increase perpendicularly to the parallel lines shown in Figure 4.3, i.e. the vulnerability increase along with the displayed arrow in the graph. Consequently, the hurricane vulnerability rank number can be assessed as shown in the graph (Figure 4.3).

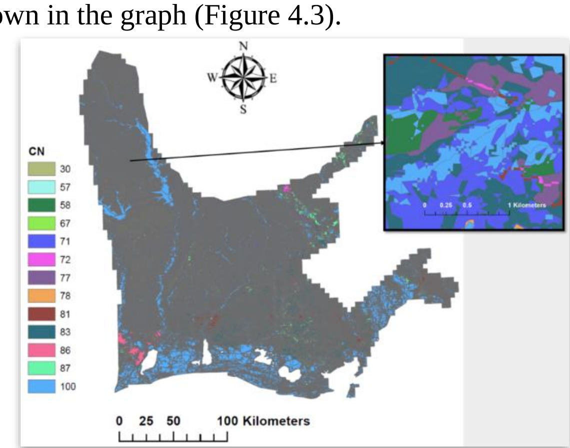

Figure 4.2: Sample of calculated NRCS-CN grid map for a region impacted by Hurricane Rita (2005).

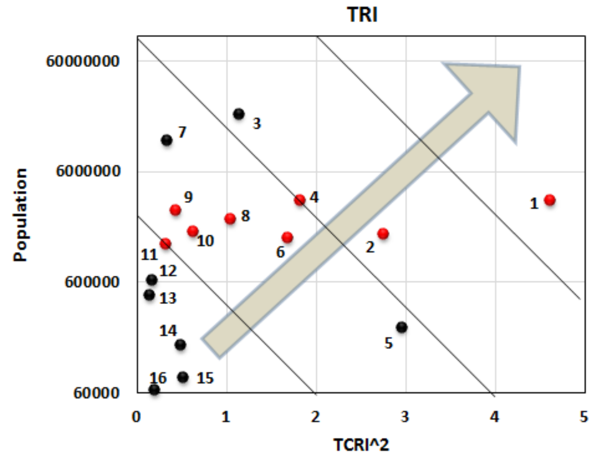

Figure 4.3: The hurricane vulnerability rank based on the population at risk and the squared TCRI. Estimated vulnerability rank is indicated by the numbers for each dot (hurricane). Red dots indicate hurricanes impacting areas with a similar population.

The Root Mean Square Error (RMSE) in the rank position of hurricanes has been calculated for both damage and death toll scenarios. Table 4.2 shows that combining the population and the TRI as in figure 4.3 yields a lower RMSE in rank position, at 3.5 and 2.2, compared with the SSHS at 5.8 and 5.7, respectively.

Table 4.2: The SSHS and TRI RMSE comparison.

RMSE in Rank Position		
	Damage	Death Toll
TRI	3.5	2.2
SSHS	5.8	5.7

There is a cluster of hurricanes in Figure 4.3 with roughly the same population at risk (red dots). The TCRI for this subset of hurricanes has been plotted against damage and death toll (Figure 4.4) to better identify other potential parameters. In both the damage and death toll cases, a threshold is recognizable (dash line in Figure 4.4 a,b), and above these thresholds, these data show significant correlations with TCRI [18].

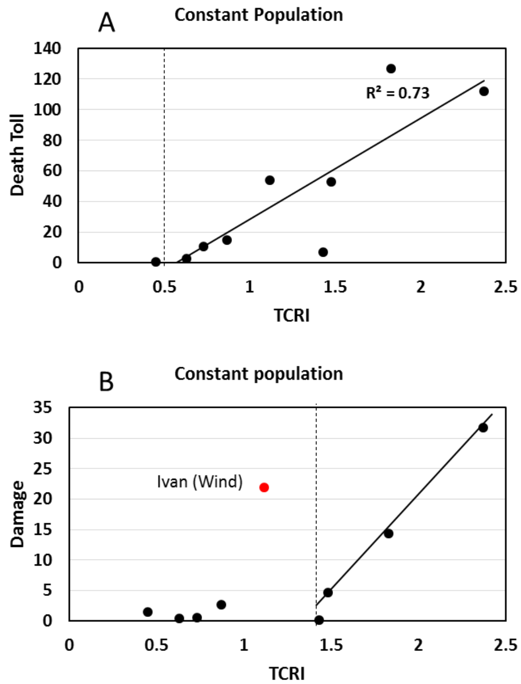

Figure 4.4: The relation between TCRI and hurricane damage and death toll in the case of near constant population at risk.

When TCRI is constant, there is no detectable correlation between population and damage or death toll, which demonstrates that wind and storm surge are important. Thus, it is necessary to pursue a similar approach for wind, and storm surge as individual tropical cyclone hazard components. However, difficulties arise since there is only limited data available for each hurricane hazard. A more detailed analysis of the causes of fatalities follows in the next section.

5. Conclusion and Discussion

The methodology has been developed to assess the vulnerability of land in the case of freshwater flooding caused by hurricane rainfall. The land-use type, hydrological soil type, and elevation map have been considered as the hydrological effective factors for the estimation of the NRCS-CN, as well as taking into account the population at risk of each hurricane as the exposure of the hazard.

Two comparison examples have been presented to explain the role of the land characteristics on vulnerability; hurricane Frances (2004) versus hurricane Jeanne (2004), and hurricane Rita (2005) versus hurricane Irene (2011).

These results show that the impacted area Curve Number of hurricanes Frances and Jeanne are approximately the same which is logically predictable due to their similar trajectories. The reason for differences between their damage and death toll despite the differences in their rainfall characteristics might be due to the significant difference in the number of residents at risk (impacted population). Hurricane Frances affected more than 11 million residents with a population density of 130 people per square kilometre versus approximately half a million residents with a population density of 32 people per square kilometre for Jeanne.

The same calculations have been performed for CAT3 hurricane Rita and CAT2 hurricane Irene to support the theory that the population at risk is the most important indicator of freshwater flood vulnerability, between those indicators which were considered in this study. These results indicate that the areas impacted by Rita have greater runoff potential than Irene. However, ignoring any differences in emergency management decisions and evacuation systems, the degree of exposure might also be the reason, since Irene impacted more than 19 million residents versus 1.6 million exposed in hurricane Rita.

6. References

1- Escudero Castillo, M., et al., (2012), *Characterization of Risks in Coastal Zones: A Review.* Clean - Soil, Air, Water. 40(9): p. 894-905.

2- Tran, P. and R. Shaw, (2017), *Towards an integrated approach of disaster and environment management*: A case study of Thua Thien Hue province, central Viet Nam. Environmental Hazards. 7(4): p. 271-282.

3- van der Weide, J., (1993), *A systems view of integrated coastal management.* Ocean and Coastal Managemen. 21(1-3): p. 129-148.

4- Peduzzi, P., et al., (2012), *Global trends in tropical cyclone risk.* Nature Climate Change. 2(4): p. 289-294.

5- Dao, H. and P. Peduzzi, (2004), Global evaluation of human risk and vulnerability to natural hazards., in Enviro-info. Geneve. p. 435-446.

6- Davidson, R. and K. Lambert, (2001), *Comparing the Hurricane Disaster Risk of U.S. Coastal Counties.* Natural Hazards Review. 2(3): p. 132-142.

7- Alwang, J., P.B. Siegel, and S.L. Jorgensen, (2001), *Vulnerability: a view from different disciplines*, Social protection discussion paper series.

8- Peduzzi, P., et al., (2009), *Assessing global exposure and vulnerability towards natural hazards; the Disaster Risk Index.* Natural Hazards and Earth System Sciences (NHESS). 9(4): p. 1149-1159.

9- Bo, X., et al., (2011), Application of the SCS-CN model to runoff estimation in a small watershed with high spatial heterogeneity. Pedosphere. 21(6): p. 738-749.

10- Greene, R. and J. Cruise, (1995), *Urban watershed modeling using geographic information system.* Journal of water resources planning and management. 121(4): p. 318-325.

11- Mishra, S., et al., (2006), *SCS-CN-based modeling of sediment yield.* Journal of Hydrology. 324(1): p. 301-322.

12- Tsihrintzis, V.A. and R. Hamid, (1997), *Urban Stormwater Quantity/Quality Modeling Using The Scs*

[DOR: 20.1001.1.23456000.2020.13.0.4.6]

Method And Empirical Equations1. JAWRA Journal of the American Water Resources Association. 33(1): p. 163-176.
13- Agriculture, U.S.D.o., (1986), *Urban Hydrology for Small Watershed. Technical Release (TR-55)(Second Edition)*. p. Conservation Engineering: Natural Resource Conservation service.
14- Homer, C.G., et al., (2015), *Completion of the 2011 National Land Cover Database for the conterminous United States-Representing a decade of land cover change information.* Photogrammetric Engineering and Remote Sensing. v. 81, no. 5: p. p. 345-354.
15- Center for International Earth Science Information Network - CIESIN - Columbia University and Centro Internacional de Agricultura Tropical - CIAT, *Gridded Population of the World, Version 3 (GPWv3): Centroids*. 2005, NASA Socioeconomic Data and Applications Center (SEDAC): Palisades, NY.
16- Jarvis, A., H.I. Reuter, A. Nelson, E. Guevara, (2008), *Hole-filled SRTM for the globe Version 4*, available from the CGIAR-CSI SRTM 90m Database.
17- Czajkowski, J., K. Simmons, and D. Sutter, (2011), *An analysis of coastal and inland fatalities in landfalling US hurricanes.* Natural Hazards. 59(3): p. 1513-1531.
18- Rezapour, M. and T.E. Baldock, (2014), *Classification of Hurricane Hazards: The Importance of Rainfall.* Weather and Forecasting. 29(6): p. 1319-1331.

[DOR: 20.1001.1.23456000.2020.13.0.4.6]